Interaction of the Pore-Forming Protein Equinatoxin II with Model Lipid Membranes: A Calorimetric and Spectroscopic Study[†]

Nataša Poklar,*[,‡] Jure Fritz,[‡] Peter Maček,[§] Gorazd Vesnaver,[‡] and Tigran V. Chalikian[||]

Department of Chemistry and Biochemistry, University of Ljubljana, Aškerčeva 5, 1000 Ljubljana, Slovenia, Department of Biology, University of Ljubljana, Večna pot 111, 1000 Ljubljana, Slovenia, and Department of Pharmaceutical Sciences, Faculty of Pharmacy, University of Toronto, 19 Russell Street, Toronto, Ontario, Canada M5S 2S2

Received July 12, 1999; Revised Manuscript Received September 13, 1999

ABSTRACT: The interactions of equinatoxin II (EqTxII) with zwitterionic (DPPC) and anionic (DPPG) phospholipids and an equimolar mixture of the two phospholipids (DPPC/DPPG) have been investigated by differential scanning calorimetry (DSC), CD−spectropolarimetry, intrinsic emission fluorescence spectroscopy, and ultrasonic velocimetry. EqTxII binds to small unilamellar vesicles formed from negatively charged DPPG lipids, causing a marked reduction in the cooperativity and enthalpy of their gel/liquid-crystalline phase transition. This transition is completely abolished at a lipid-to-protein ratio, L/P, of 10. For the mixed DPPC/DPPG vesicles, a 2-fold greater lipid-to-protein ratio (L/P = 20) is required to abolish the phase transition, which corresponds to the same negative charge (−10) of lipid molecules per EqTxII molecule. The disappearance of the phase transition of the lipids apparently corresponds to the precipitation of the lipid−protein complex, as suggested by our sound velocity measurements. Based on the far-UV CD spectra, EqTxII undergoes two structural transitions in the presence of negatively charged vesicles (DPPG). The first transition coincides with the gel/liquid-crystalline phase transition of the lipids, which suggests that the liquid-crystalline form of negatively charged lipids triggers structural changes in EqTxII. The second transition involves the formation of α-helical structure. Based on these observations, we propose that, in addition to electrostatic interactions, hydrophobic interactions play an important role in EqTxII−membrane association.

Interactions between membranes and proteins are of central importance for the proper insertion and folding of membrane proteins, the breaching of membrane barriers by toxins, the action of antibiotic peptides, and the interaction of hormones with membrane receptors (*1*). A common feature of membrane−protein interactions is the partitioning of the protein between water and a lipid bilayer (*1*). How proteins can be posttranslationally transferred across or inserted into membranes remains a puzzling and controversial issue. In one scenario, insertion of some protein toxins into membranes requires interactions of the membrane surface with protein groups that are more readily accessible in the partially folded state (e.g., molten globule) as opposed to the native state (*2*, *3*). This hypothesis, while plausible, still needs to be corroborated experimentally. In fact, to the best of our knowledge, the formation of a membrane-bound molten globule has not been detected experimentally yet. Moreover, according to one recent study, the membrane-bound conformation of the colicin E1 channel domain is an expanded two-dimensional helical array and not a molten globule (*4*).

Proteins which are capable of changing their water/membrane solubility in response to changes in their environment offer a unique opportunity to study the processes associated with protein−membrane association and insertion. The characterization of membrane-induced structural changes in proteins is important for a better understanding of the mode of action of these proteins. In addition, such a characterization may provide insights into the mechanisms by which membrane−protein interactions modulate protein structure.

Equinatoxin II, a 179 amino acid residue cytolysin from *Actinia equina* L., is a pore-forming protein found in sea anemones. It has an isoelectric point of 10.5 and a molecular mass of 19.8 kDa (*5*, *6*). As we have recently shown, EqTxII[1] assumes a molten globule conformation at low pH and high temperature (*7*, *8*). The stability of the molten globule state of EqTxII at high temperatures is strongly salt dependent. In addition, EqTxII undergoes two sequential conformational transitions at alkaline pH (N. Poklar, unpublished results).

[†] This work was supported by the Slovene Science Foundation (PZIT-0029-98 to N.P.) and by a NATO Collaborative Linkage Grant (LST.CLG 974812 to T.V.C.).

* To whom correspondence should be addressed at the Department of Chemistry and Biochemistry, University of Ljubljana, Aškerčeva 5, 1000 Ljubljana, Slovenia. Fax: +38661 1254458. E-mail: natasa.poklar@uni-lj.si.

[‡] Department of Chemistry and Biochemistry, University of Ljubljana.

[§] Department of Biology, University of Ljubljana.

[||] Department of Pharmaceutical Sciences, University of Toronto.

[1] Abbreviations: EqTxII, equinatoxin II; DPPC, L-α-dipalmitoylphosphatidylcholine; DPPG, L-α-dipalmitoylphosphatidylglycerol; DPPC/DPPG, vesicles prepared from an equimolar mixture of DPPC and DPPG lipids; CD, circular dichroism; DSC, differential scanning calorimetry; L/P, lipid-to-protein ratio; SUV, small unilamellar vesicle(s); MLV, multilamellar vesicle(s); Δ*H*, enthalpy of the lipid phase transition; T_m, transition temperature.

10.1021/bi9916022 CCC: $18.00
Published on Web 10/23/1999

The first base-induced transition of EqTxII is accompanied by a partial loss of secondary and tertiary structures, while the second base-induced transition involves a complete loss of tertiary structure with the formation of non-native α-helical structure (N. Poklar, unpublished results). Although the mechanisms of pore formation of EqTxII and other eukaryotic toxins are not fully understood at the molecular level, pore formation is considered to be a multistep process. Specifically, it has been proposed that pore formation is initiated by the binding of EqTxII monomers to the membrane (*9*), followed by insertion of the monomers into the membrane, and, finally, by oligomerization of the monomers within the membrane to form functional pores (*10*). We have proposed that the conformational transitions of EqTxII observed under mild denaturing conditions in the absence of lipids (e.g., the native-to-molten globule transition and the formation of additional α-helical secondary structure) may correlate with the ability of EqTxII to bind to lipid membranes and form cation-selective pores (*10*).

To further explore the interactions of EqTxII with lipid membranes and to determine the role of protein structure in lipid−protein interactions, we now expand our studies to include interactions of EqTxII with small unilamellar lipid vesicles: zwitterionic L-α-dipalmitoylphosphatidylcholine (DPPC), anionic L-α-dipalmitoylphosphatidylglycerol (DPPG), and the equimolar mixture of these lipids. To this end, we have used a wide variety of experimental techniques, including differential scanning calorimetry (DSC), CD−spectropolarimetry, intrinsic emission fluorescence spectroscopy, and sound velocity measurements, to investigate the gel/liquid-crystalline phase transitions in the protein−lipid complexes and the structural/conformational changes in EqTxII associated with protein−lipid interactions.

MATERIALS AND METHODS

Preparation of Lipid Vesicles. L-α-Dipalmitoylphosphatidylcholine (DPPC) and L-α-dipalmitoylphosphatidylglycerol (DPPG) were purchased from Sigma Chemical Co. (St. Louis, MO) and used without further purification. Suspensions of lipid vesicles for DSC, CD−spectropolarimetry, and intrinsic emission fluorescence measurements were prepared as follows. Pure DPPC and DPPG lipids (5 mg) were dissolved in 10 mL of chloroform and in a chloroform:methanol = 3:1 mixture, respectively. Equimolar mixtures of DPPG (M_w = 745.0) and DPPC (M_w = 734.0) lipids were prepared by mixing the two lipid solutions to a molar ratio of 1:1. All lipid solutions were dried by slow evaporation under a constant flow of nitrogen. Following the removal of the last traces of solvent in a vacuum, triply distilled water was added to the lipids to give a final concentration of 3.0 mg/mL. Multilamellar vesicles (MLV) were prepared by vortexing the lipid suspension for 10 min. MLV were further transformed to small unilamellar vesicles (SUV) by sonication using an ultrasonic disintegrator (150 W) equipped with a microprobe until the milky MLV suspension became clear (approximately 10 min on ice). The lipid concentrations for DSC and CD measurements were between 0.5 and 1 mg/mL. Fluorescence titration experiments were performed at a lipid concentration of about 1 mg/mL, while a concentration of about 3 mg/mL was used for sound velocity measurements.

Preparation of the Protein Solution. EqTxII was isolated from the sea anemone *Actinia equina* L. as previously described (*5*), lyophilized, and stored as a powder at −10 °C. EqTxII solutions for the near- and far-UV CD measurements and for DSC measurements were prepared directly by dissolving the protein in triply distilled water ($c \approx 1$ mg/mL) and were further diluted by addition of liposome solution to the appropriate lipid-to-protein ratio. Protein solutions for sound velocity measurements were dialyzed overnight against triply distilled water, and the concentration was determined spectrophotometricaly at 20 °C using an extinction coefficient of $\epsilon_{280\ nm}$ = 1870 mL/(g·cm). For fluorescence titration experiments, EqTxII solutions (c = 0.01 mg/mL) were prepared before each experiment by diluting the aqueous stock solution with triply distilled water.

Differential Scanning Calorimetry. DSC experiments were performed using a Setaram Micro-DSC Calorimeter (Setaram, Caluire, France) as described previously (*11*). Removable sample and reference cells with an optimal operational volume of 0.8 mL were used. The calorimeter was calibrated by means of the Joule effect using special cells (*11*). DSC melting profiles for DPPC, DPPG, and an equimolar mixture of DPPC and DPPG lipids in water and in the presence of EqTxII at lipid-to-protein molar ratios (L/P) of 100:1 and 20:1 were recorded over the temperature range from 20 to 60 °C at a constant heating rate of 0.5 °C/min. The corresponding base lines had been obtained using cells filled with the same amount of the solvent and were subsequently subtracted from the lipid/protein thermograms. The melting temperature, T_m, and the transition enthalpy, ΔH, were determined from the first DSC scan (*11*), while the second scan was used to assess the reversibility of the phase transition.

Circular Dichroism (CD) Spectropolarimetry. CD experiments were performed using an AVIV model 62A DS spectropolarimeter (Aviv Associates, Lakewood, NJ) equipped with a thermoelectrically controlled cell holder. The far-UV CD spectra of EqTxII at different molar ratios of added lipids (L/P = 100:1 to 10:1) were recorded using a 0.25 mm path length quartz cuvette. At all L/P ratios employed, the absolute lipid concentration was kept constant to ensure a constant contribution from light scattering to the recorded CD spectra. The CD spectra were recorded at 5 °C intervals in the temperature range from 5 to 95 °C. All spectra were "baseline-corrected", smoothed by a polynomial fitting function (Aviv Associates, Inc.), and converted to mean residue ellipticity, $[\Theta]_\lambda$, as follows:

$$[\Theta]_\lambda = \frac{M_0 \Theta_\lambda}{100cl} \qquad (1)$$

where $M_o = M_w/N$; M_w is the molecular weight of the protein; N is the number of amino acid residues; Θ_λ is the ellipticity in degrees; c is the concentration in grams per milliliter; and l is the path length in decimeters.

Intrinsic Emission Fluorescence Measurements. All emission fluorescence measurements were performed using a Perkin-Elmer model LS-50 luminescence spectrometer with a water-thermostated cell holder using a 1 cm path length quartz cuvette. Slit widths with a nominal band-pass of 5 nm were used for both excitation and emission beams. Excitation wavelengths of 280 and 293 nm were used, and

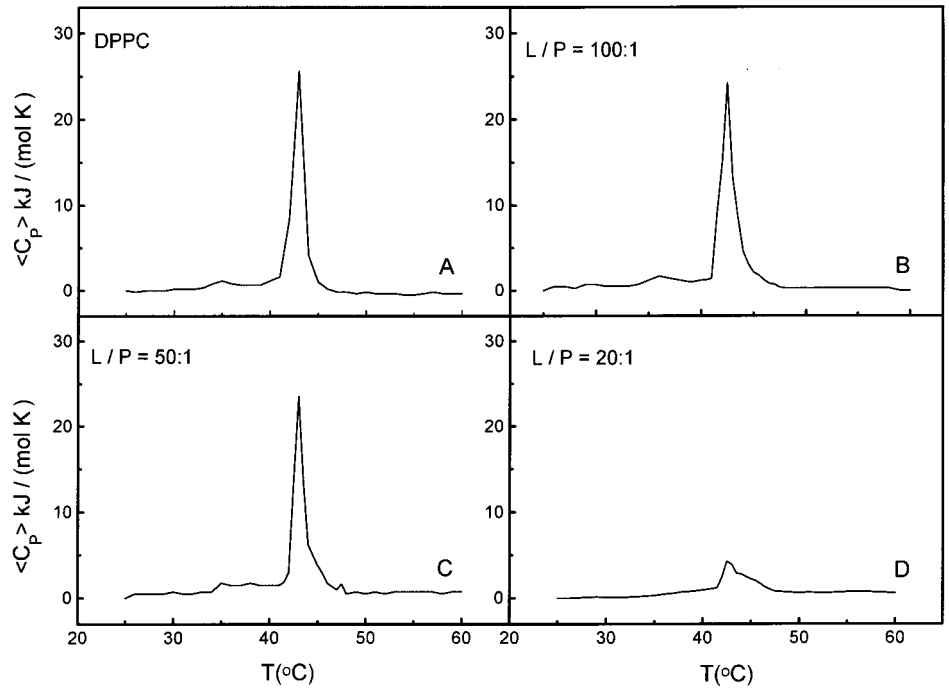

FIGURE 1: Apparent excess heat capacity curves of DPPC vesicles in water and at different lipid-to-EqTxII ratios, L/P. (A) DPPC vesicles alone, $c_{DPPC} = 1$ mg/mL; (B) L/P = 100:1, $c_{DPPC} = 1$ mg/mL and $c_{EqTxII} = 0.27$ mg/mL; (C) L/P = 50:1, $c_{DPPC} = 1$ mg/mL and $c_{EqTxII} = 0.54$ mg/mL; (D) L/P = 20:1, $c_{DPPC} = 0.5$ mg/mL and $c_{EqTxII} = 0.67$ mg/mL.

the emission spectra were recorded in the range 300−500 nm. Isothermal titration experiments of aqueous solutions of EqTxII with DPPC and DPPG liposomes were performed at 25 and 48 °C by incremental addition of 2.5−50 μL aliquots of 1 mg/mL lipids into the initial 2 mL solution of 0.01 mg/mL (5.0×10^{-7} M) EqTxII. After each addition, the emission spectrum was recorded. An identical procedure was used in the absence of EqTxII to obtain the emission spectra of pure solvent (background intensity), which was subtracted from the corresponding emission spectra of EqTxII. The emission spectra of EqTxII were multiplied by a dilution factor and corrected for PM-tube response using a fluorescence spectrum of quinine sulfate ($c = 2.5 \times 10^{-7}$ M) in 0.1 M perchloric acid as a standard. The temperature in the cell was measured with an Fe/Fe−constantan thermocouple.

Ultrasonic Velocimetry. Solution sound velocity measurements were performed at 7.5 MHz using a previously described resonator method (*12*−*14*). We used an ultrasonic resonator cell with lithium niobate piezo transducers and a sample volume of 0.8 mL (*13*). For this type of acoustic resonator, the relative precision of the sound velocity measurements at frequencies near 7.5 MHz is at least $\pm 1 \times 10^{-4}$ % (*15*, *16*). The characteristic property of a solute derived directly from ultrasonic measurements is the relative specific sound velocity increment, [u]:

$$[u] = \frac{\Delta u}{u_o c} = \frac{u - u_o}{u_o c} \qquad (2)$$

where c is the specific concentration of a solute expressed in grams per milliliter; u and u_o are the sound velocities in the solution and the solvent, respectively. Acoustic titration experiments were performed by adding equal quantities of a 3 mg/mL lipsome solution to both the sample and the reference cells filled with 0.8 mL of a protein solution (0.5 mg/mL) and water, respectively. Initial volumes of a protein solution (in the sample cell) and water (in the reference cell) were delivered via a 1 mL Hamilton syringe equipped with a Chaney adapter, while the titrant additions were made via 10 or 50 μL Hamilton syringes equipped with a Chaney adapter (Hamilton Co., Reno, NV). In calculating the relative specific sound velocity increment, [u], we took into account changes in the sound velocity in the solvent, u_o, and in the concentration of the solute, c, that result from addition of the lipid solution. The change in the sound velocity relative increment, $\Delta[u]$, associated with protein−lipid interactions was calculated using the equation:

$$\Delta[u] = (u_{P+L} - u_{B+L})(1 + V'/V'_o)/(u_{B+L}c) - [u]_o \quad (2a)$$

where u_{P+L} is the sound velocity in a solution formed by adding a liposome solution with a volume of V' into a protein solution with a volume of V'_o; u_{B+L} is the sound velocity in a solution formed by adding a liposome solution with a volume of V' into a buffer solution with a volume of V'_o; c is the initial concentration of the protein; $[u]_o$ is the relative specific sound velocity increment of the initial lipid-free protein.

RESULTS

Differential Scanning Calorimetry. Figure 1 shows the DSC melting profiles of zwitterionic DPPC vesicles in water in the absence and presence of EqTxII at various lipid-to-protein (L/P) ratios. In the absence of EqTxII, DPPC exhibits two endothermic transitions at 35 and 43 °C, respectively (Figure 1A, Table 1). The first transition at 35 °C corresponds to the melting of the lipid headgroups. The second transition at 43 °C corresponds to the highly cooperative gel/liquid-crystalline (chain melting) transition of the lipid side chains. The enthalpy, ΔH, of the gel/liquid-crystalline transition of

Table 1: Gel/Liquid-Crystalline Transition Enthalpies, ΔH, for DPPC, DPPG, and Mixed DPPC/DPPG Vesicles and the Corresponding Transition Temperatures, T_m, at Different Lipid-to-EqTxII (L/P) Ratios As Obtained from DSC

	ΔH (kJ/mol)	T_m (°C)
DPPC	39 ± 4	43.0 ± 0.5
L/P = 100:1	39 ± 4	43.0 ± 0.5
L/P = 50:1	36 ± 4	42.5 ± 0.5
L/P = 20:1	9 ± 4	42.5 ± 0.5
DPPG	30 ± 4	46.0 ± 0.5
L/P = 100:1	27 ± 4	45.5 ± 0.5
L/P = 50:1	23 ± 4	45.5 ± 0.5
L/P = 20:1	4 ± 4	45 ± 1
DPPC/DPPG	35 ± 4	47 ± 1
L/P = 100:1	34 ± 4	45 ± 1
L/P = 50:1	28 ± 4	43 ± 1

DPPC equals 39 kJ/mol, in good agreement with literature values ranging from 36 to 43 kJ/mol (*17*, *18*). At high lipid-to-protein ratios, that is, at low protein concentrations, the chain melting transition of DPPC is not affected by EqTxII (see Figure 1B,C and Table 1). This observation suggests that the interactions of EqTxII with zwitterionic DPPC vesicles do not alter significantly the packing of hydrocarbon chains in the gel and liquid-crystalline states. However, at high concentrations of EqTxII (L/P is 20:1), the chain melting transition of DPPC practically disappears (Figure 1D, Table 1). It should be noted that the shape of the thermograms and the ΔH values obtained from the second temperature scan of the same sample do not change, suggesting that the phase transition of DPPC is reversible at all L/P ratios.

Figure 2 (panels A−D) shows the DSC melting profiles of anionic DPPG vesicles in the presence and absence of EqTxII. As is seen from Figure 2A, DPPG exhibits a single endothermic transition at 46.0 °C, which corresponds to the highly cooperative gel/liquid-crystalline phase transition of the lipid. For this transition, we measure an enthalpy change, ΔH, of 30 kJ/mol, in good agreement with the literature value of 33 kJ/mol (*19*). When EqTxII is added to the lipid solution, the thermodynamics at DPPG melting change dramatically. At low concentrations of EqTxII (L/P is between 100:1 and 50:1), the ΔH value of DPPG melting decreases significantly. It should be noted that, as revealed by our previous studies (*7*, *8*), ExTxII undergoes a heat-induced denaturation within the same temperature range. Therefore, our determined value of ΔH should reflect the gel/liquid-crystalline transition of DPPG vesicles and the heat-induced denaturation of the protein, as well as the change in nature of protein/lipid interactions before and after the transition. At higher concentrations of the protein (L/P is 10:1), the transition disappears completely (see Figure 2D). To account for this observation, we propose that EqTxII interacts with anionic DPPG vesicles, thereby changing the packing of the hydrocarbon chains. At all L/P ratios, the values of ΔH for the DPPG melting transition calculated from the first and the second runs coincide; however, the two thermograms differ in shape.

Figure 3 (panels A−D) shows the DSC melting profiles for the 1:1 binary mixture of DPPG and DPPC vesicles in the presence and absence of EqTxII. The enthalpy, ΔH, of chain melting of the DPPG/DPPC vesicles in water is 35 kJ/mol at a T_m of 47.0 °C. Note that the transition enthalpy, ΔH, for the binary DPPC/DPPG vesicles is higher than that for pure DPPG vesicles, but lower than that for pure DPPC vesicles. The transition temperature for the mixed DPPG/DPPC vesicles is similar to that for pure DPPG vesicles. At low to moderate concentrations of EqTxII (L/P = 100:1 and 50:1), the T_m of the chain melting transition of DPPC/DPPG vesicles decreases, while the transition enthalpy, ΔH, does not significantly change (Figure 3B,C, Table 1). At high concentrations of the protein (L/P is 20:1), the chain melting transition disappears (see Figure 3D). Thermograms obtained

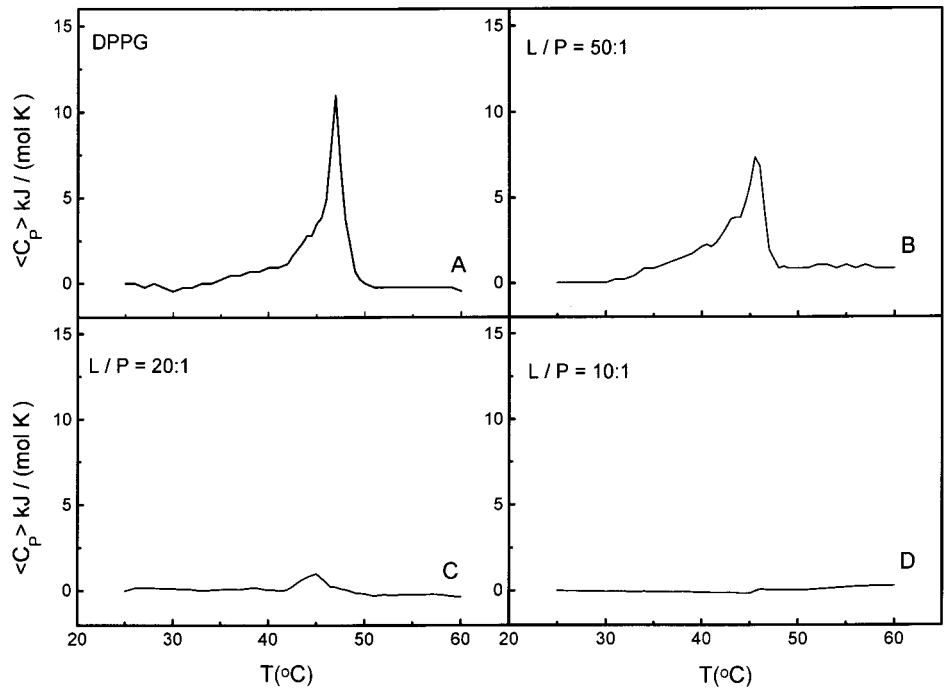

FIGURE 2: Apparent excess heat capacity curves of DPPG vesicles in water and at different lipid-to-EqTxII ratios, L/P. (A) DPPG vesicles alone, c_{DPPG} = 1 mg/mL; (B) L/P = 100:1, c_{DPPG} = 1 mg/mL and c_{EqTxII} = 0.27 mg/mL; (C) L/P = 50:1, c_{DPPG} = 1 mg/mL and c_{EqTxII} = 0.54 mg/mL; (D) L/P = 10:1, c_{DPPG}= 0.25 mg/mL and c_{EqTxII} = 0.73 mg/mL.

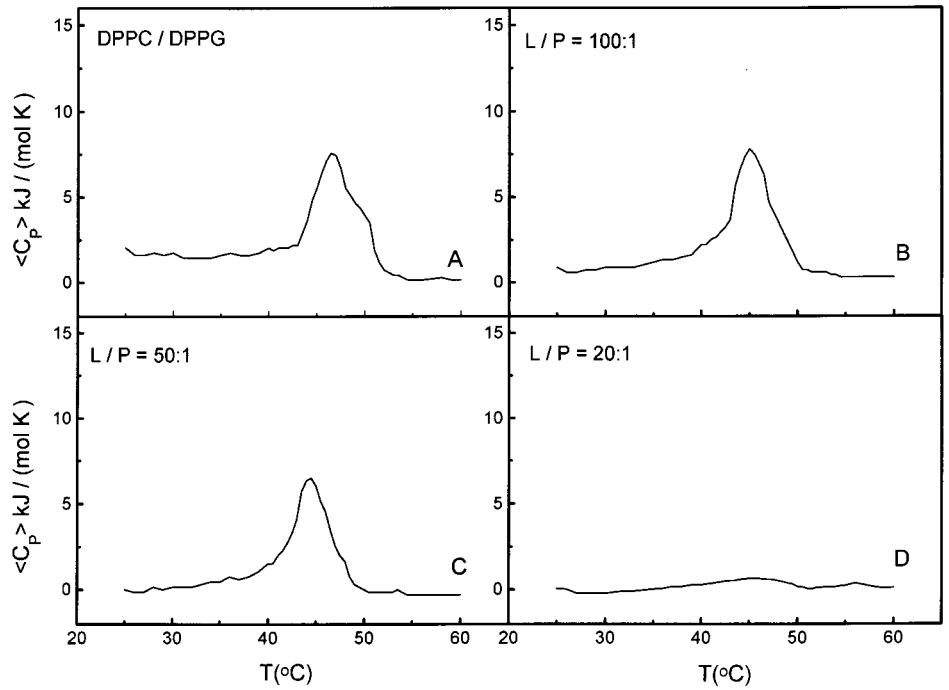

FIGURE 3: Apparent excess heat capacity curves of an equimolar mixture of DPPC/DPPG vesicles in water and at different lipid-to-EqTxII ratios, L/P. (A) DPPC/DPPG vesicles alone, $c_{DPPC/DPPG} = 1$ mg/mL; (B) L/P = 100:1, $c_{DPPC/DPPG} = 1$ mg/mL and $c_{EqTxII} = 0.27$ mg/mL; (C) L/P = 50:1, $c_{DPPC/DPPG} = 1$ mg/mL and $c_{EqTxII} = 0.54$ mg/mL; (D) L/P = 20:1, $c_{DPPC/DPPG} = 0.5$ mg/mL and $c_{EqTxII} = 0.67$ mg/mL.

by rescanning the samples result in approximately the same values of T_m and ΔH, while the cooperativity of each transition decreases.

For the DPPC/DPPG vesicles, the gel/liquid-crystalline phase transition disappears at a L/P ratio of about 20:1, while for pure DPPG vesicles, this transition disappears at a L/P ratio of about 10:1. As suggested by Lakey et al. (*20*), the disappearance of the gel/liquid-crystalline phase transition at high protein concentrations is related to the opening of the compact protein structure and the unmasking of the hydrophobic groups in the protein molecules. If the amount of lipid is insufficient to cover all unmasked hydrophobic groups, protein−protein interactions cause precipitation of the protein (*20*). According to some other studies, association of proteins with lipids can result in the aggregation of protein-containing lipid vesicles (*21*), the formation of extended lipid structures, and/or vesicle fusion (*22*, *23*).

CD−Spectropolarimetry. Figure 4 presents the far-UV CD spectra of the EqTxII/DPPC mixtures recorded at 25, 60, 70, 80, and 95 °C at L/P ratios of 100:1 (panel A) and 20:1 (panel B). The CD melting profiles at 208, 217, and 235 nm measured for L/P of 100:1 and 20:1 are shown in panels C and D, respectively. Since pure lipids do not exhibit any CD signal between 200 and 250 nm, the CD spectra shown in Figure 4 predominantly reflect the structural/conformational properties of EqTxII. Below 60 °C, at all L/P ratios, the CD spectra of EqTxII in DPPC solution and pure water are identical (*8*). Each of these spectra has a characteristic minimum at 217 nm, indicative of proteins rich in β-sheets. Above 60 °C, the CD spectra shown in Figure 4 are consistent with the loss of secondary structure of EqTxII.

At L/P ratios of 100:1 (see Figure 4C) and 50:1 (not shown), the transition temperature, T_m, determined from the CD melting profiles at 208, 217, and 235 nm is 68 ± 1 °C. At higher protein concentrations (e.g., at an L/P ratio of 20:1), the T_m is equal to 70 ± 1 °C (see Figure 4D). Note that at L/P ratios of 100:1 and 50:1, the posttransitional shape (e.g., at 80 and 95 °C) of the far-UV CD spectrum of EqTxII is quite similar to that in the absence of lipids (*8*). By contrast, at higher protein concentrations (e.g., at an L/P ratio of 20:1), the posttransitional shape of the far-UV CD spectrum of the protein is significantly different from that in the absence of lipids (see Figure 4A,B).

Figure 5 (panels A and B) shows the far-UV CD spectra of EqTxII in the presence of DPPG at different L/P ratios at 25, 50, 85, and 95 °C. In the presence of DPPG vesicles, the characteristic minimum of the native EqTxII spectrum is red-shifted from 217 nm in water to 220 nm. Our CD melting profiles shown in Figure 5 allow us to identify two distinct heat-induced transitions of EqTxII. At an L/P of 100:1 (see Figure 5C), the first transition monitored by the ellipticity at 235 nm occurs at 50 °C, while the second transition monitored by the ellipticity at 208 and 217 nm occurs around 80 °C. However, the second transition, which results in the formation of an α-helical structure, is not complete even at our highest experimental temperature of 95 °C. For L/P ratios of 50:1 (Figure 5B) and 20:1 (not shown), at high temperatures (80 and 95 °C), the characteristic α-helical minimum at 222 nm becomes less pronounced, although the two transitions with T_m values of 50 and 80 °C still can be detected (Figure 5D). At a L/P ratio of 10:1, reliable CD measurements become impossible due to the turbidity of the solution at all temperatures. Recall that, for this L/P value, our DSC data reveal the absence of any cooperative transition. The observed red shift in the position of the minima and the disappearance of the CD signal at high protein concentration (at low L/P ratios) could be due to the absorption flattening effect. This effect results from the nonrandom distribution of protein chromophores and becomes important only in SUV at low L/P ratios (*24*).

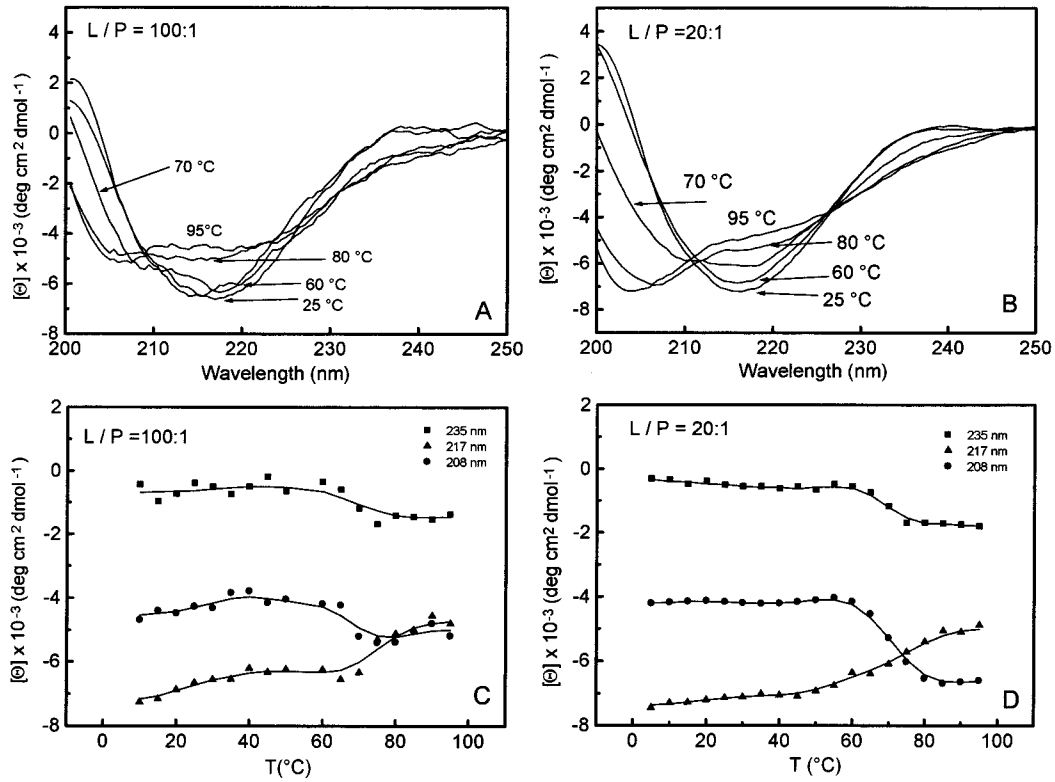

FIGURE 4: Far-UV CD spectra of EqTxII in the presence of zwitterionic DPPC vesicles at different lipid-to-protein ratios (L/P) at 25, 60, 70, 80, and 95 °C and the corresponding CD melting profiles followed at 235 (■), 217 (▲), and 208 (●) nm. (A, C) L/P = 100:1, c_{DPPC} = 1 mg/mL and c_{EqTxII} = 0.27 mg/mL; (B, D) L/P = 20:1, c_{DPPC} = 0.5 mg/mL and c_{EqTxII} = 0.67 mg/mL.

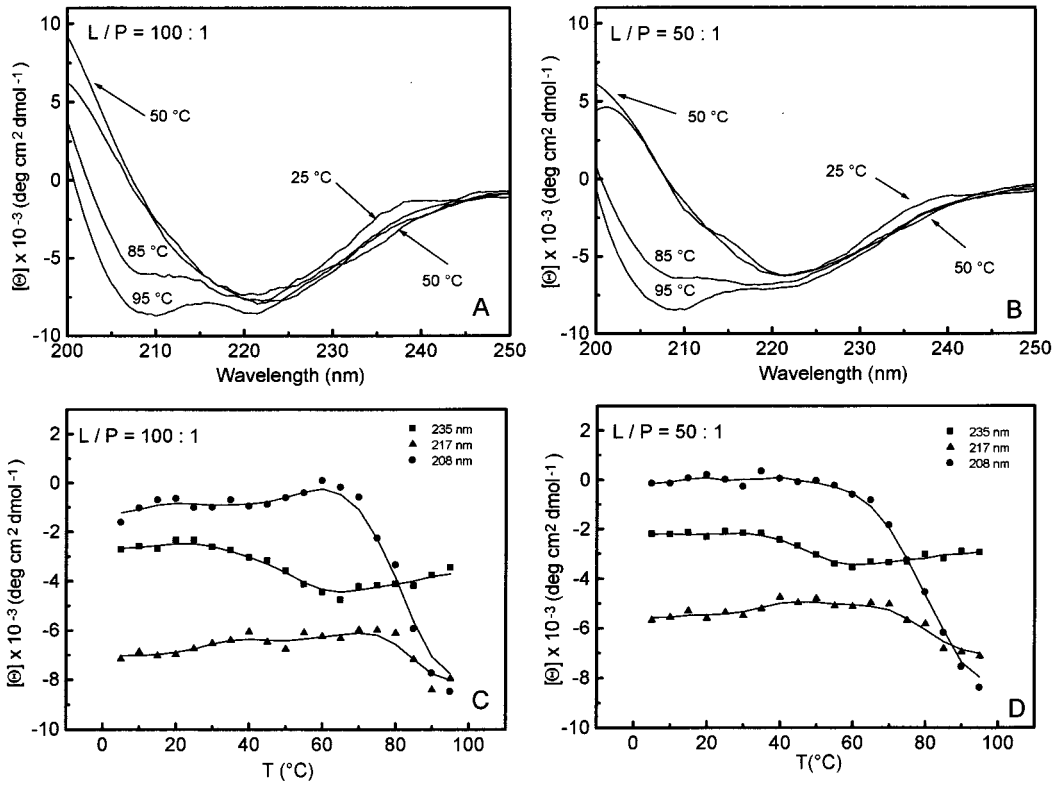

FIGURE 5: Far-UV CD spectra of EqTxII in the presence of anionic DPPG vesicles at a few selected temperatures at different lipid-to-protein ratios (L/P) at 25, 50, 85, and 95 °C and the corresponding CD melting profiles followed at 235 (■), 217 (▲), and 208 (●) nm. (A, C) L/P = 100:1, c_{DPPG} = 1 mg/mL and c_{EqTxII} = 0.27 mg/mL; (B, D) L/P = 50:1, c_{DPPG} = 1 mg/mL and c_{EqTxII} =0.54 mg/mL.

Figure 6 (panels A and B) shows the far-UV CD spectra of EqTxII in the presence of mixed DPPC/DPPG vesicles at different values of L/P at 25, 50, 85, and 95 °C. At an L/P of 20:1, CD measurements are not possible due to protein precipitation. At the highest L/P ratio of 100:1, the far-UV CD spectrum of EqTxII in the presence of DPPC/DPPG vesicles is different from that of EqTxII in the presence of pure DPPC (Figure 4) or pure DPPG (Figure 5). Neverthe-

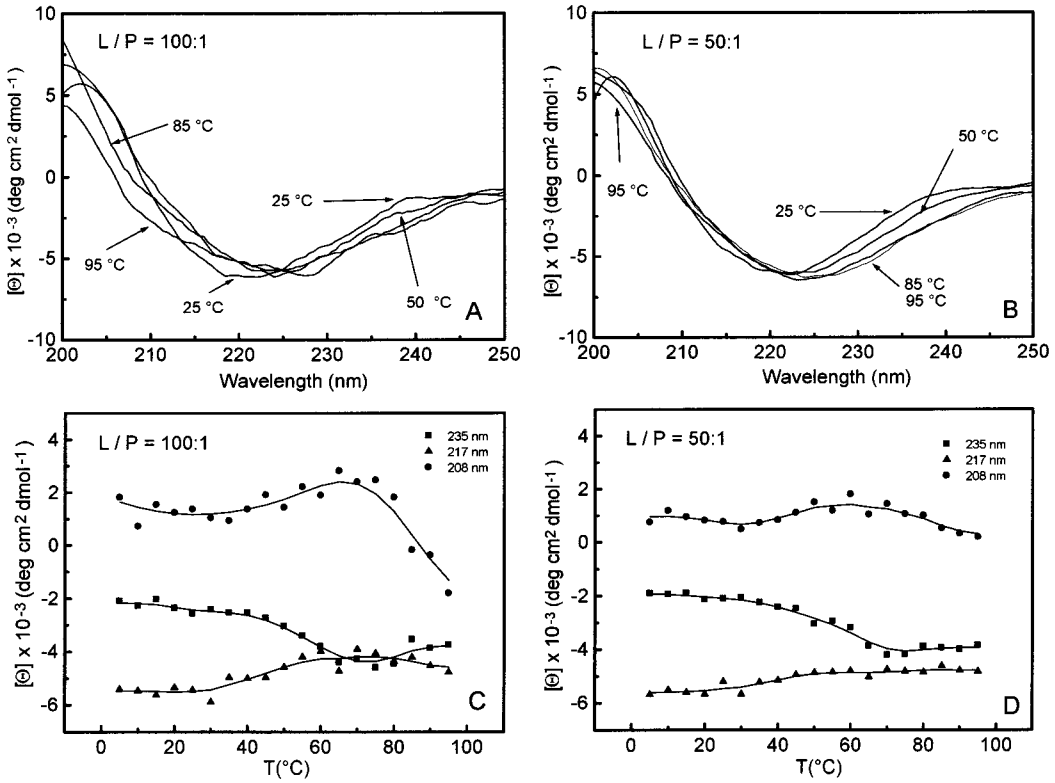

FIGURE 6: Far-UV CD spectra of EqTxII in the presence of an equimolar mixture of DPPC/DPPG lipids at different lipid-to-protein ratios (L/P) at 25, 50, 85, and 95 °C and the corresponding CD melting profiles followed at 235 (■), 217 (▲), and 208 (●) nm. (A, C) L/P = 100:1, $c_{DPPC/DPPG}$ = 1 mg/mL and c_{EqTxII} = 0.27 mg/mL; (B, D) L/P = 50:1, $c_{DPPC/DPPG}$ = 1 mg/mL and c_{EqTxII} = 0.54 mg/mL.

less, CD melting profiles at 208, 217, and 235 nm detect two distinct transitions at 50 and 80 °C for L/P ratios of 100:1. The first transition at 50 °C can be monitored by the ellipticity at 217 and 235 nm, while the second transition at 80 °C can be monitored by the ellipticity at 208 nm. Note that at an L/P of 50:1, the second transition becomes less pronounced.

In summary, our CD results suggest that at high L/P ratios the thermal denaturation of EqTxII in the presence of DPPG or DPPC/DPPG vesicles occurs in two distinct steps. The first transition occurs in the temperature range corresponding to the phase transition of pure DPPG or DPPC/DPPG vesicles. Probably, this transition involves the exposure of some protein hydrophobic groups to the melted chains in the hydrocarbon core of the membrane while leaving the secondary structure largely unaltered (*25*). The second transition above 70 °C is still incomplete at 95 °C and involves the formation of non-native α-helical secondary structure. Both transitions of EqTxII in the presence of mixed DPPC/DPPG lipids occur at temperatures slightly higher than in the presence of DPPG lipids.

Intrinsic Emission Fluorescence. Figure 7 shows the intrinsic fluorescence intensity of EqTxII as a function of the L/P ratio at 25 and 48 °C (below and above the gel/liquid-crystalline phase transition temperature for DPPC or DPPG lipids). Note that, at 25 °C, quenching of the fluorescence emission intensity of EqTxII is quite similar for DPPC and DPPG vesicles. By contrast, at 48 °C, the magnitude of quenching in the presence of DPPG vesicles is more pronounced than in the presence of DPPC vesicles (Figure 7). However, at either temperature, there is no shift in the position of the λ_{max} (332 nm ± 1 nm) of the emission

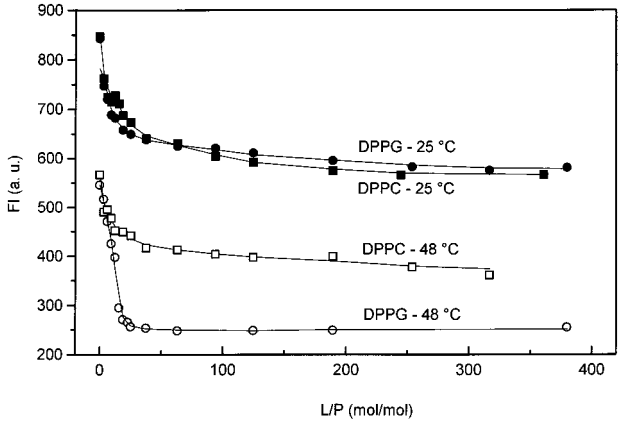

FIGURE 7: Intrinsic emission fluorescence intensity, FI, at λ_{em} = 333 nm, of EqTxII (c_{EqTxII} = 0.01 mg/mL) titrated by DPPC (■, □) and DPPG (●, ○) vesicles (c_{lipids} = 1 mg/mL) at 25 °C (solid symbols) and 48 °C (open symbols), λ_{exc} = 280 nm.

fluorescence spectra of the protein in the presence of DPPC or DPPG vesicles. Stronger quenching of the EqTxII emission fluorescence at 48 °C in the presence of DPPG relative to DPPC suggests that the protein fluorophores are in close proximity or, even, in direct contact with the negatively charged DPPG headgroups (*26*). The absence of any shift in the position of the fluorescence emission maximum in the presence of lipids implies that when EqTxII binds to lipid vesicles, the overall polarity of the fluorophore microenvironment remains unchanged. This may suggest that, at these temperatures, neither an insertion of the EqTxII aromatic residues into the lipid nor a change in protein conformation occurs.

Relative Specific Sound Velocity Increment. Figure 8 shows the change in the relative specific sound velocity

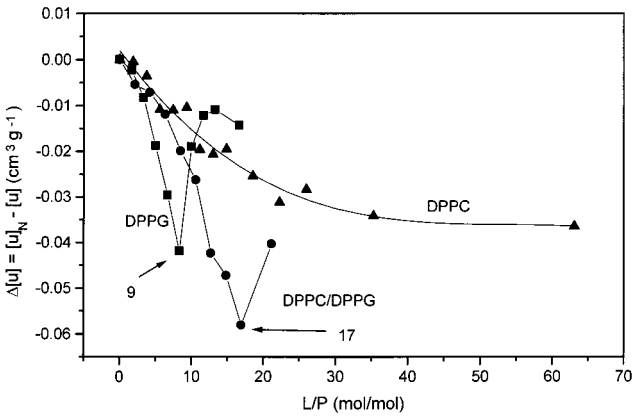

FIGURE 8: Change in the relative specific sound velocity increment, $\Delta[u]$, for EqTxII ($c_{EqTxII} = 0.5$ mg/mL) as a function of increased lipid-to-protein ratio, L/P, at 25 °C for DPPC (▲), DPPG (■), and mixed DPPC/DPPG (●) lipids ($c = 3$ mg/mL). $[u]_N$ and $[u]$ stand for the relative specific sound velocity increment of EqTxII in triply distilled water and in the presence of lipids, respectively.

increment, $\Delta[u]$, of EqTxII upon addition of DPPC, DPPG, or mixed DPPC/DPPG vesicles to the protein solution at 25 °C. Inspection of Figure 8 reveals that the relative specific sound velocity increment, $[u]$, of the protein monotonically decreases when the concentration of DPPC increases within the whole range of L/P studied here. By contrast, in the presence of DPPG or mixed DPPC/DPPG lipids, after an initial gradual decrease followed by a sharp decrease, the value of $[u]$ sharply increases. This perturbation is due to the aggregation of the protein−lipid complexes, which occurs for DPPG and DPPC/DPPG vesicles at L/P ratios of 9 ± 1 and 17 ± 1, respectively. These results are in qualitative agreement with our CD measurements where the same L/P ratios have been determined for the aggregation of the two protein−lipid complexes. In addition, recall that at these L/P ratios, the thermotropic transitions of the lipids disappear as revealed by our DSC measurements.

DISCUSSION

EqTxII Belongs to the Group of Proteins Which Interact with Phospholipid Vesicles by a Combination of Electrostatic and Hydrophobic Forces. Papahadjopoulos et al. (*27*) divided proteins and polypeptides into three types according to their effect on the gel/liquid-crystalline phase transitions of phospholipids, although many membrane proteins cannot be fitted unequivocally into this scheme. According to this classification, EqTxII can be considered as a type II protein. Type II proteins, which are water-soluble and hydrophilic, are believed to interact with phospholipid bilayers by a combination of electrostatic and hydrophobic forces, initially adsorbing onto the charged polar headgroups of the phospholipids and then penetrating into the amphiphilic interface of the bilayer to interact with the lipid hydrocarbon chains. These proteins expand phospholipid monolayers, thereby increasing permeability of phospholipid vesicles. Usually, type II membrane proteins cause a decrease in the T_m, the cooperativity of the gel/liquid-crystalline phase transition, and a decrease in the transition enthalpy, ΔH. Recall that, consistent with this expectation, our DSC measurements revealed an EqTxII-induced reduction in the cooperativity and enthalpy of the gel/liquid-crystalline phase transition of the anionic DPPG lipids and a decrease in the T_m of the phase transition of the mixed DPPC/DPPG vesicles.

The Process of Binding and Inserting of EqTxII to Negatively Charged Vesicles at Neutral pH Is Triggered by the Thermotropic Phase Transition of the Lipids. All proposed models for binding of positively charged peptides and proteins to negatively charged vesicles invoke at least two steps (*28*, *29*). The first step, which involves the association of the positively charged polypeptide with the negatively charged vesicles at a bilayer surface, results in an overall charge neutralization. As revealed by our DSC and fluorescence measurements, the interactions between EqTxII and anionic DPPG vesicles and negatively charged mixed DPPC/DPPG vesicles are stronger than that between EqTxII and zwitterionic DPPC vesicles. Apparently, the initial binding of EqTxII involves electrostatically driven protein−lipid association at the bilayer surface. The second step in the protein−membrane interactions is the hydrophobic adsorption of the protein at the membrane, caused by the partial penetration of the hydrophobic amino acid side chains into the lipid bilayer (*28*, *29*). The adsorption can involve protein penetration into the headgroup region only, or penetration into the hydrophobic core of the lipid bilayer. The importance of this step in determining EqTxII interactions with anionic vesicles is underscored by the increase in protein α-helicity when interacting with lipids in their liquid-crystalline state (see Figure 5). Apparently, the insertion of positively charged EqTxII into the negatively charged lipid vesicles at neutral pH is triggered by the thermotropic phase transition of the lipids and the toxin. Since the far-UV CD spectrum and the intrinsic fluorescence emission of the toxin do not change at temperatures below the lipid phase transition, we propose that EqTxII does not penetrate into the bilayer in the gel state. By contrast, at higher temperatures, the thermally induced conformational transition of EqTxII in the presence of negatively charged DPPG or DPPC/DPPG vesicles coincides with the phase transition of DPPG or DPPC/DPPG vesicles. The formation of non-native α-helix-rich secondary structure indicates that EqTxII penetrates into the lipid membranes when they are in their liquid-crystalline state and favor α-helical structures (*30*, *31*). These interpretations are in agreement with previous observations that EqTxII emission fluorescence intensity increases and the emission spectrum is blue-shifted in the presence of egg phosphatidylcholine SUV and that the permeability of calcein-loaded vesicles increases when sphingomyelin is introduced into the vesicles (*32*, *10*). The structural changes occurring during the gel/liquid-crystalline phase transitions of lipids have also been observed for other membrane proteins and peptides such as *Escherichia coli* SecA protein (*33*), cytochrome *c* (*21*), and the small synthetic model hydrophobic peptide Lys_2-Gly-Leu_{24}-Lys_2-Ala-amide, P_{24} (*34*). In fact, the very fact that such structural changes do occur suggests that, under appropriate conditions, significant changes in the conformation of hydrophobic peptides or proteins may be induced by changes in the physical state or thickness of the lipid bilayer (*34*).

Formation of an Amphiphilic α-Helical Structure. Recall that our CD measurements revealed that at high temperatures, when anionic lipids are in their liquid-crystalline state, the α-helical content of EqTxII increases. This increase is more pronounced at higher ratios of DPPG to EqTxII (L/P > 20). It should be noted that the α-helical structure is thermodynamically favored for an isolated or noninteracting polypep-

tide chain in the hydrophobic core or in the integral layer of the membrane (*30*, *31*). In general, peptides and proteins that bind to membranes are amphiphilic in nature, with the distribution of charged and hydrophobic residues in accord with the periodicity of the helix turn. The N-terminal 13−20 amino acid region of EqTxII is amphiphilic in nature (*35*) and, thus, is very likely to adopt an α-helical form when located within the lipid bilayer. The tryptophan-rich 105−120 region, as well as aliphatic groups of Ser160 and Arg144, can also be involved in the interactions with lipid membranes (*36*).

EqTxII Concentration Effect. EqTxII (*10*) and some other peptides such as marginin 2 amide (*37*) and wheat α-thionin (*38*) apparently perform their pore-forming functions only at low L/P ratios. Regarding EqTxII−membrane interactions, it should be noted that, at low L/P ratios, protein-bound vesicles aggregate, which is a rather common phenomenon (*20*, *21*, *37*). One may propose that the electrostatic nature of peptide−lipid interactions, as can be predicted based on some models (*39*), is crucial only for the initial binding of the protein to the vesicle surface. Aggregation of such complexes, however, must involve further electrostatic as well as hydrophobic interactions within the protein−vesicle complexes (*38*).

CONCLUDING REMARKS

We have used differential scanning calorimetry to determine the influence of the pore-forming toxin EqTxII on the thermotropic phase transitions of small unilamellar vesicles prepared from zwitterionic DPPC, anionic DPPG, and their equimolar mixture. Furthermore, we have employed CD spectropolarimetry and intrinsic emission fluorescence spectroscopy to monitor the lipid-induced conformational changes in EqTxII. Our results suggest the following general features: (i) The binding of EqTxII to lipids results in a decrease in the enthalpy of the heat-induced phase transition of anionic vesicles and has no effect on the transition of zwitterionic vesicles at low protein concentrations. (ii) Two conformational transitions of EqTxII can be identified at elevated temperatures in the presence of anionic vesicles, while in the presence of zwitterionic vesicles there is only one conformational transition. (iii) The first conformational transition of EqTxII in the presence of anionic lipids coincides with the thermotropic phase transition of the lipids. The second protein transition involves the formation of pronounced α-helical structure and occurs at high L/P ratios and high temperatures when lipids are in their liquid-crystalline form. (iv) Aggregation occurs at low L/P ratios. The differences in the behavior of EqTxII in the presence of different lipids indicate that EqTxII has a preference for anionic lipids in the liquid-crystalline form.

This report represents the first step toward establishing a thermodynamic database needed to gain insights into the molecular forces that govern the binding of EqTxII to lipid membranes. In this context, the next logical step is to characterize thermodynamically the binding of EqTxII to natural lipids in their liquid-crystalline state.

ACKNOWLEDGMENT

We thank Prof. Dr. Polona Čadež (Department of Food Technology, University of Ljubljana) for permitting us to use an ultrasonic disintegrator equipped with microprobe. We are especially grateful to Dr. Jens Völker (Rutgers, The State University of New Jersey, Piscataway, NJ) for critical reading of the manuscript and many helpful suggestions.

REFERENCES

1. White, S. H., and Wimley, W. C. (1994) *Curr. Opin. Struct. Biol. 4*, 79−86.
2. Bychkova, V. E., Pain, R. H., and Ptitsyn, O. B. (1988) *FEBS Lett. 238*, 231−234.
3. Ptitsyn, O. B. (1995) *Adv. Protein Chem. 47*, 83−229.
4. Zakharov, S. D., Linderberg, M., Griko, Y., Tollin, G., Prendergast, F. G., and Cramer, W. A. (1998) *Proc. Natl. Acad. Sci. U.S.A. 95*, 4282−4284.
5. Maček, P., and Lebez, D. (1988) *Toxicon 26*, 441−445.
6. Maček, P. (1992) *FEMS Microbiol. Immunol. 105*, 121−130.
7. Malavašič, M., Poklar, N., Maček, P., and Vesnaver, G. (1996) *Biochim. Biophys. Acta 1280*, 65−72.
8. Poklar, N., Lah, J., Salobir, M., Maček, P., and Vesnaver, G. (1997) *Biochemistry 36*, 14345−14352.
9. Zorec, R., Tester, M., Maček, P., and Mason, W. T. (1990) *J. Membr. Biol. 118*, 243−249.
10. Belmonte, G., Pederzolli, C., Maček, P., and Manestrina, G. (1993) *J. Membr. Biol. 131*, 11−22.
11. Lapanje, S., and Poklar, N. (1989) *Biophys. Chem. 34*, 155−162.
12. Eggers, F., and Funck, Th. (1973) *Rev. Sci. Instrum. 44*, 969−978.
13. Sarvazyan, A. P. (1982) *Ultrasonics 20*, 151−154.
14. Eggers, F. (1992) *Acustica 76*, 231−240.
15. Sarvazyan, A. P., Selkov, E. E., and Chalikian, T. V. (1988) *Sov. Phys. Acustic. 34*, 631−634.
16. Sarvazyan, A. P., and Chalikian, T. V. (1991) *Ultrasonics 29*, 119−124.
17. Bach, D., and Chapman, D. (1980) in *Biological Microcalorimetry* (Beezer, A. E., Ed.) pp 275−309, Academic Press, New York.
18. Blume, A. (1983) *Biochemistry 22*, 5436−5442.
19. McElhaney, R. N. (1986) *Biochim. Biophys. Acta 864*, 361−421.
20. Lakey, J. H., Massotte, D., Heitz, F., Dasseux, J.-L., Faucon, J.-F., Parker, M. W., and Pattus, F. (1991) *Eur. J. Biochem. 196*, 599−607.
21. Heimberg, T., and Biltonen, R. L. (1994) *Biochemistry 33*, 9477−9488.
22. Kim, J., and Kim, H. (1986) *Biochemistry 25*, 7867−7874.
23. Pécheur, E.-I., Sainte-Marie, J., Bienvenue, A., and Hoekstra, D. (1999) *Biochemistry 38*, 364−373.
24. Wallace, B. A., and Teeters, C. L. (1987) *Biochemistry 26*, 65−70.
25. Van der Goot, F. G., Lakey, J. H., and Pattus F. (1992) *Trends Cell Biol. 2*, 343−348.
26. González-Mañas, J. M., Lakey, J. H., and Pattus, F. (1993) *Eur. J. Biochem. 211*, 625−633.
27. Papahadjopoulos, D., Moscarello, M., Eylar, E. H., and Isac, T. (1975) *Biochim. Biophys. Acta 401*, 317−335.
28. Varanda, W., and Finkelstein, A. (1980) *J. Membr. Biol. 55*, 203−211.
29. Schender, S. L., and Cramer, W. A. (1994) *Protein Sci. 3*, 2272−2279.
30. Engelman, D. M., and Steitz, T. A. (1981) *Cell 23*, 411−422.
31. Jacobs, R. E., and White, S. H. (1989) *Biochemistry 28*, 3421−3437.
32. Maček, P., Zecchini, M., Pederzolli, C., Dalla Serra, M., and Manestrina, G. (1995) *Eur. J. Biochem. 234*, 329−335.
33. Ulbrandt, N. D., London, E., and Oliver, D. B. (1992) *J. Biol. Chem. 267*, 15184−15192.
34. Zhang, Y., Lewis, R. N. A. H., McElhaney, R. N., and Ryan, R. O. (1992) *Biochemistry 31*, 3942−3952.

35. Belmonte, G., Menestrina, G., Pederzolli, C., Križaj, I., Gubenšek, F., Turk, T., and Maček, P. (1994) *Biochim. Biophys. Acta*. *1192*, 197−204.
36. Anderluh, G., Barlič, A., Podlesek, Z., Maček, P., Pungerčar, J., Gubenšek, F., Zecchini, M. L., Dalla Serra, M., and Menestrina, G. (1999) *Eur. J. Biochem. 263*, 128−136.
37. Wenk, M. R., and Seelig, J. (1998) *Biochemistry 37*, 3909−3916.
38. Caaveiro, J. M. M., Molina, A., Rodríguez-Palenzuela, P., Goñi, F. M., and González-Mañas, J. M. (1998) *Protein Sci. 7*, 2567−2577.
39. Murray, D., Hermida-Matsumoto, L., Buser, C. A., Tsang, J., Sigal, C. T., Ben-Tal, N., Honig, B., Resh, M. D., and McLaughlin, S. (1998) *Biochemistry 37*, 2145−2159.

BI9916022